# On the microstructural refinement in commercial purity Al and Al-10wt.% Cu alloy under ultrasonication during solidification

H.R. Kotadia[1], M. Qian[2], D.G. Eskin[3,4] and A. Das[5*]

[1] Warwick Manufacturing Group, The University of Warwick, Coventry CV4 7AL, UK

[2] School of Engineering, RMIT University, Melbourne, VIC 3000, Australia

[3] Brunel Centre for Advanced Solidification Technology, Brunel University London, Uxbridge UB8 3PH, UK

[4]Tomsk State University, Tomsk 634050, Russia

[5] College of Engineering, Swansea University Bay Campus, Fabian Way, Swansea, SA1 8EN, UK

**Abstract:**

Physical grain refinement is examined under high-intensity ultrasonication during solidification in commercial purity Al (CP-Al) and binary Al-10wt.% Cu alloy melts cooled naturally in air and compared against chemical inoculation using Al-5Ti-1B grain refiner. The coarse dendritic unrefined base microstructure was completely replaced with a fine equiaxed grain structure in the case of either inoculation or ultrasonication. However, ultrasonication produced more effective refinement over chemical inoculation with a two-fold and eight-fold increase in the grain density in CP-Al and Al-10%Cu alloy, respectively. While combining chemical inoculation with ultrasonication produced the finest grain structure in CP-Al, no further improvement over ultrasonication was noted for the Al-10%Cu alloy. Noticeable reduction in nucleation undercooling, of similar magnitude to chemical inoculation, was observed under ultrasonication. Cooling curve observations indicate strongly enhanced heterogeneous nucleation under ultrasonication. It appears that although the potency of nucleants is higher under chemical inoculation, more nucleation events are favoured under cavitation.

***Keywords:*** Grain refining; Ultrasound; Cavitation; Al-Ti-B refiner; Aluminium alloys; Solidification microstructure

* Corresponding author. Tel.: +44 1792 602031 E-mail address: a.das@swansea.ac.uk (A. Das)

## 1. Introduction

Chemical grain refinement is widely practiced for Al [1, 2] and Mg [3] castings to promote equiaxed grain formation and refine ingot or billet grain structures. Motivation for such refinement is to reduce hot tearing, porosity and segregation, enhance microstructural homogeneity, and to improve mechanical properties of as-cast components [4, 5]. The effectiveness of a specific grain refiner, however, is often dependent on the alloy composition. Some of the industrially important alloys respond poorly to established refiners. For example, Zr is the preferred grain refiner for Mg-alloys but is largely ineffective in Al-containing Mg-alloys [3]. Similarly, Al-5Ti-1B master alloy is the most popular inoculant for Al-alloys but is least effective in Al-alloys containing high amounts of Si [5, 6]. Even for successful chemical inoculation, the grain refining efficiency is known to deteriorate with melt holding prior to casting (known as the 'fading effect') [7]. Drastic reduction in refining performance (known as the 'poisoning effect') is also observed from certain alloying elements [8]. In addition, potent nucleating particles can be susceptible to agglomeration [9]. Accumulation of agglomerates of nucleants in the finished castings can pose limitations for critical applications where the inclusion content needs to be kept to a minimum.

An emerging alternative to addressing the inherent limitations of chemical inoculation is to apply a physical field such as high-intensity mechanical shear [10], electromagnetic field [11], electric current pulse [12], or low frequency mechanical vibration [13] during solidification. Among the various physical refinement techniques, application of high-intensity ultrasound has shown promising grain refinement results for Mg-alloys [14-16], Al-alloys [14, 17-19], and TiAl alloys [20]. Direct introduction of ultrasound into the melt during solidification could be an alternative grain refinement approach to inoculation for relatively low-melting alloys. The evolution of solidification microstructure under ultrasonication is generally explained on the basis of non-linear phenomena caused by high-intensity sound wave propagation through the melt [14, 21]. Such phenomena are predominantly cavitation and acoustic streaming.

Above the cavitation threshold, formation, growth and collapse of tiny gas bubbles in the liquid is stated to produce shockwave pulses of 1000 atm and local microjects of 100 $ms^{-1}$ [18]. Acoustic streaming, resulting from the attenuation of ultrasound in the melt, promotes large and small-scale steady fluid flow [21]. Although the origin of microstructural refinement is largely attributed to the cavitation phenomena, the exact mechanism(s) of such refinement is still debated. It is argued that shockwaves generated through cavitation fragment the dendrite arms, and the fluid flow resulting from

acoustic streaming disperses the fragments in the bulk melt leading to copious nucleation [17, 21-22]. Partial melting and detachment of secondary dendrite arms is also possible due to the increased fluid flow and mass transfer around the solid-liquid interface. But these mechanisms can only act when ultrasonication is performed below the liquidus. When the melt is processed above the liquidus, it is suggested that grain refinement results from enhanced nucleation on wet insoluble inclusions [18, 23]. The enhanced wetting of non-metallic particles under ultrasonication has been demonstrated in oxide containing metal matrix composite [24]. Chalmers discussed nucleation under cavitation based on two different mechanisms; evaporative cooling at the cavitation bubble surface and pressure induced displacement of the equilibrium temperature (from Clapeyron equation) [25]. He rejected the former mechanism on theoretical grounds suggesting that nucleation is unlikely as the total cooling possible during the life of a bubble is limited. The idea of nucleation occurring at the existing liquid temperature was considered most likely due to displacement of the equilibrium temperature under the high-pressure pulse generated by collapsing cavitation bubbles. This view on ultrasonic enhanced nucleation was supported by others [15, 26].

It appears that despite the observed influence on microstructural refinement, detailed understanding of the effects of ultrasonication on microstructure formation is still lacking. Moreover, there are only a few studies on the efficiency of ultrasonic induced refinement compared to the established practice of chemical refinement under similar solidification conditions. In the present investigation, commercial purity Al (CP-Al) and a model Al-10%Cu alloy (all compositions expressed in wt.% unless otherwise stated) is used to explore grain refinement under ultrasonication and compare against chemical inoculation. Finally, an attempt is made to identify the origin of microstructure refinement in ultrasonicated melts.

## 2. Experimental

CP-Al (99.7% purity) and Al-10% Cu alloy prepared by melting appropriate amounts of CP-Al and Cu (99.9%) were used for the solidification experiments. Al-10%Cu was chosen as a model alloy to compare ultrasonication effects in a pure metal against a simple alloy with reasonable solute content. Varying the Cu content in Al-Cu, we found the finest $\alpha$-Al grain structure to form in Al-10%Cu under conventional solidification. Accordingly, this composition was chosen for the experiments. Compositions of the metal and the alloy, as determined through optical emissions spectroscopy, are listed in table 1.

*Table 1. Composition of CP-Al and Al-10wt.%Cu alloy as determined through optical emissions spectroscopy.*

| Alloy | Elemental concentration (wt.%) | | | | |
|---|---|---|---|---|---|
| | Al | Si | Fe | Cu | Ti |
| CP-Al | balance | 0.04 | 0.082 | 0.002 | 0.004 |
| Al-10% Cu | balance | 0.04 | 0.147 | 9.8 | 0.003 |

For each batch of experiments, around 2-3 kg of pure metal or alloy was melted and homogenised for 2 h at 725 ± 3 °C in a large clay-graphite crucible held inside an electric resistance furnace. All experiments were performed using this melt reservoir to minimise compositional variation between individual experiments. For each experiment, melt was taken from the reservoir in clay-graphite crucibles (height 70 mm and diameter 50 mm) preheated to the melt temperature, placed on a refractory slab, and allowed to solidify under natural air cooling while undergoing ultrasonication or without processing. A schematic diagram of the experimental set up is shown in Fig. 1.

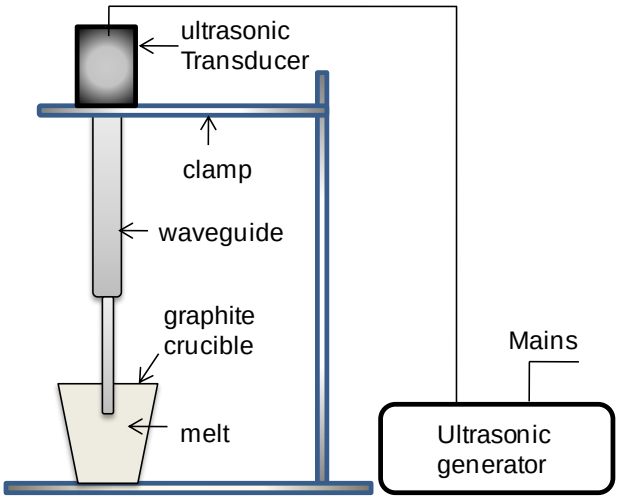


*Fig. 1. Schematic illustration of the experimental setup for direct ultrasonic treatment of solidifying melt.*

The ultrasonic system consisted of an air-cooled piezoelectric 20 kHz 0.5 kW transducer and a waveguide system. A Ti-6Al-4V alloy radiator of 25 mm diameter was used to transmit the ultrasound into the melt at maximum amplitude of 25 μm. For all the ultrasonication experiments, the radiator

(horn) was first preheated by sonicating a batch of aluminium melt (that was discarded) to prevent any chill effect. A thermocouple was placed just below the submerged horn at the centre of the ingot and the cooling curves were recorded using a multichannel data logging system. In the case of the alloy, the horn was introduced in the melt from the top at a melt temperature of 690 $^{o}$C and withdrawn at an approximate melt temperature of 545-550 $^{o}$C following around 420 s of application of ultrasound. For the CP-Al the ultrasound horn was withdrawn just before the completion of solidification.

For experiments involving chemical grain refinement, a pre-measured quantity of Al-5Ti-1B master alloy rod was preheated and added to the melt at 1% level (upper limit used in industry) to ensure adequate refinement. The melt was stirred intermittently and then taken out within 20 min (to prevent any fading effect) in a preheated clay-graphite crucible and allowed to solidify under the same cooling condition as with the ultrasonication experiments. Identical grain refiner addition level was used for solidification experiments involving simultaneous application of chemical refiner and ultrasonication. For comparison, solidification experiments were repeated from the same batch of melt under identical experimental set-up and cooling conditions but without any chemical inoculation or ultrasonication of the melt. All individual experiments were conducted at least three times to ensure reproducibility.

Solidified ingots (50 mm diameter and 60 mm height) were sectioned along the central vertical plane. Both sections were ground and polished through standard metallographic techniques, and anodized using Barker's reagent (7 ml 48% $HBF_4$ in 200 ml distilled water) at 20 VDC for 70 s using a stainless steel cathode. A ZEISS Axioscop2 MAT optical microscope equipped with an automated Zeiss AxioVision image analyser was used under polarised light for microstructural investigation. Grain size was measured using a linear intercept methods and the statistical analysis of the results was performed.

## 3. Results

### *3.1 Solidification microstructure in the CP-Al ingots*

Macrostructures of CP-Al ingots solidified from 725 $^{o}$C under different melt treatment but identical cooling conditions are presented in Fig. 2. The base unrefined microstructure developed in the quiet natural cooling set-up of the experiments consists of coarse columnar grain structure (Fig. 2a). The sample shown in Fig. 2b is chemically inoculated using Al-5Ti-1B master alloy. Substantial reduction in grain size and conversion to equiaxed grain structure is observed throughout the ingot.

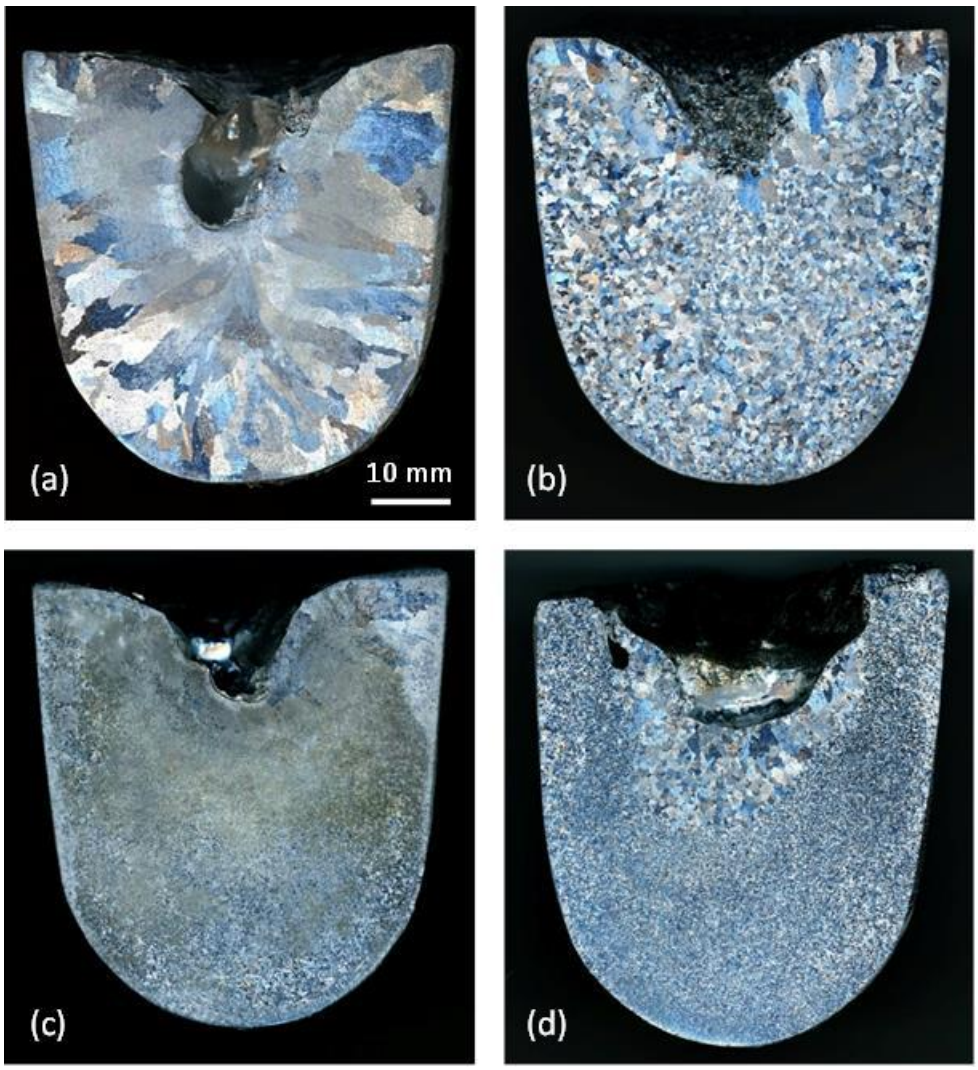


*Fig. 2. Macrostructures of commercial purity Al (CP-Al) ingots solidified from 725 $^{o}$C under identical slow cooling conditions subjected to (a) conventional solidification, (b) Al-5Ti-1B inoculation, (c) ultrasonication and (d) combined chemical inoculation and ultrasonication.*

The largest reduction in grain size is observed at the bottom of the ingot with a gradual increase in grain size towards the top of the ingot. The top of the ingot, however, shows a small region of coarser columnar grain growth. Under the slow and quiescent cooling conditions, this last liquid to solidify is thought to have limited benefit from inoculation (few nucleating particles) and columnar growth from the top surface has occurred here. As compared to inoculation, stronger microstructure refinement (finer and more uniform equiaxed grain structure) is observed when the melt is ultrasonicated without inoculation (Fig. 2c). The entire ingot has solidified under ultrasonication as the radiator was withdrawn near the completion of solidification. No coarse or columnar grains are observed at the top of the ingot as very limited remnant liquid solidified following ultrasonication. As opposed to the

chemically inoculated ingot, maximum grain refinement occurred at the top of the ingot just below the radiating face of the ultrasonic horn. Applying ultrasound to a chemically inoculated melt resulted in fine equiaxed grain structure as shown in Fig. 2d. However, a band of slightly coarser grains can be observed at the top of the ingot (Fig. 2d). This originates from early withdrawal of the ultrasound radiator leaving behind a finite volume of remnant liquid that was deliberately allowed to solidify as ultrasonication ceased. The grain structure in this coarser band is comparable to that observed in the inoculated ingot in Fig. 2b, indicating that chemical inoculation alone was responsible for grain formation in this area. It, therefore, appears that ultrasonication played the dominant role in the grain refinement observed in the ingot undergoing both chemical and physical refinement simultaneously (Fig. 2d). Fig. 2 clearly suggests a more effective microstructural refinement under ultrasonication of the solidifying melt as compared to chemical inoculation of the melt.

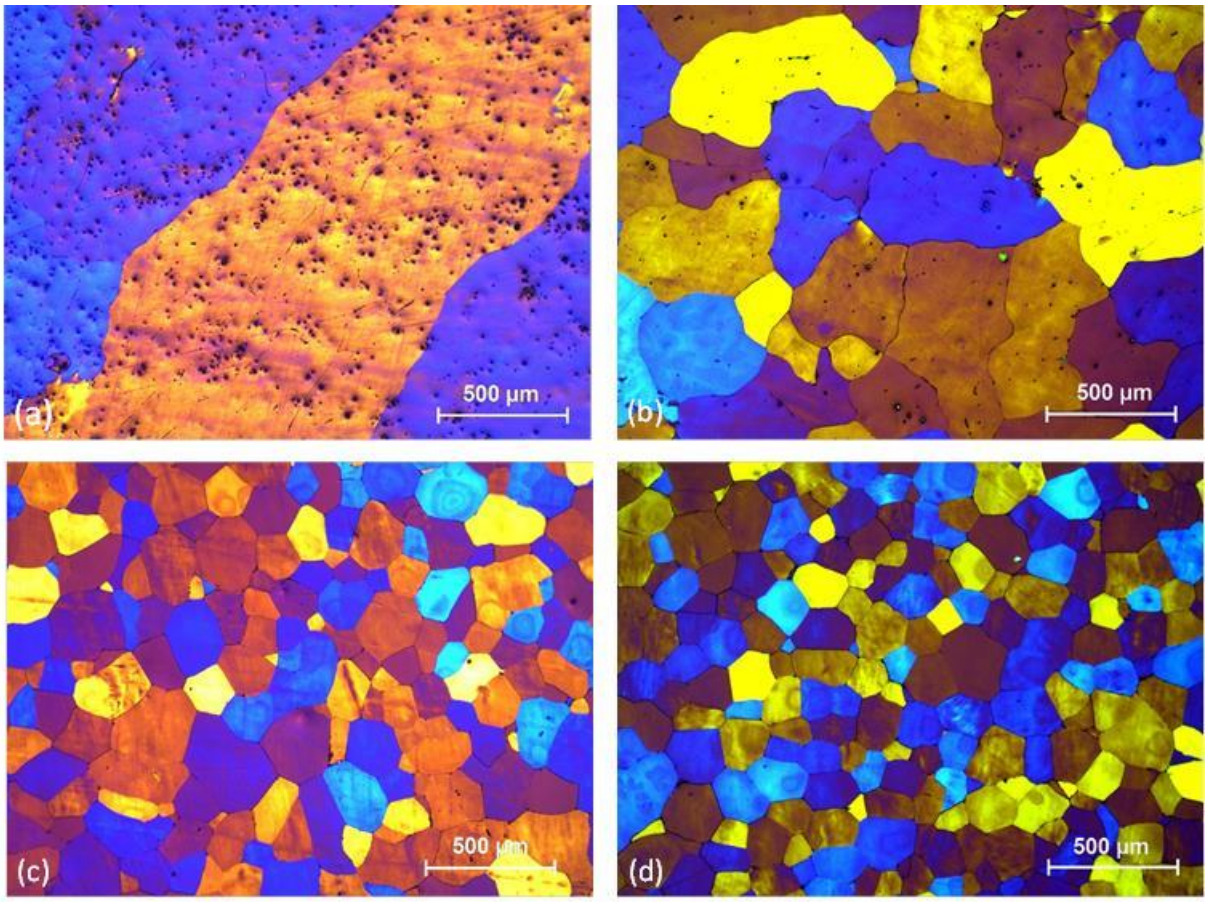


*Fig. 3. Optical micrographs of CP-Al cast from 725 $^{o}$C under identical cooling conditions subjected to (a) conventional solidification (b) Al-5Ti-1B inoculation (c) ultrasonication and (d) combined chemical inoculation and ultrasonication. Microstructures are presented from near the top of the ingots.*

Optical micrographs from the ingots shown in Fig. 2 are presented in Fig. 3 illustrating the detailed solidification grain structure formed in the respective samples. The average grain sizes along the central vertical axis from the top to the bottom of the ingot (from just below the radiator in case of ultrasonicated sample) are plotted as a function of distance in Fig. 4. Both figures 3 and 4 confirm the extent of grain refinement observed in the macrostructures of ingots solidified under chemical or physical refinement conditions.

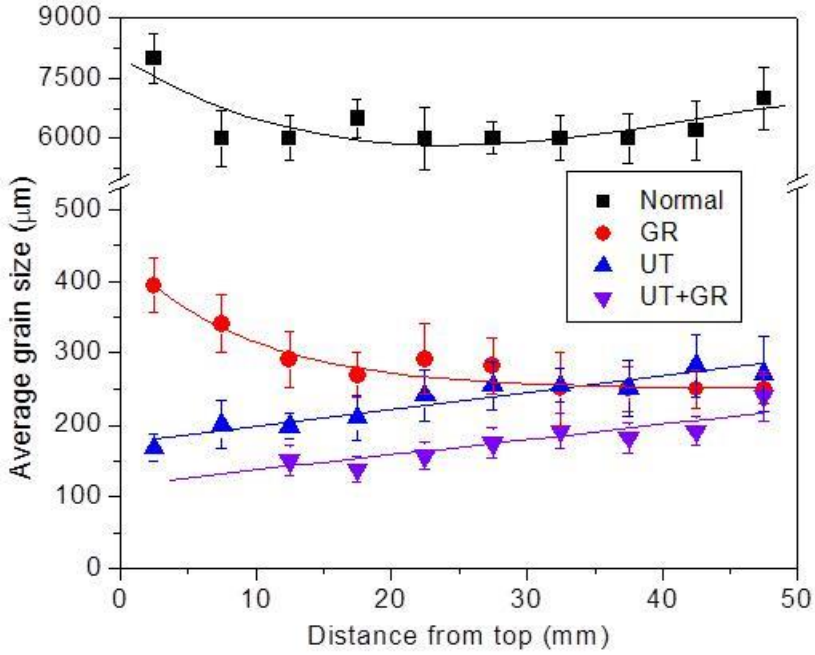


*Fig. 4. Measured average grain size for CP-Al ingots as a function of distance from the top along the central vertical axis. For ultrasonicated samples, distance is measured from the tip of the radiator.*

Without any refinement, the base microstructure consists of well-developed coarse dendritic grains (Fig. 3a) with an average grain size ranging between 6 to 8 mm in various regions of the solidified ingot. Complete conversion to fine equiaxed grain structure is observed following chemical refiner addition (Fig. 3b) with an average grain size varying from 395 ±38 μm at the top of the ingot to 250 ±21 μm near the bottom edge of the ingot where the finest grains formed. It should be noted that despite 1% addition the refining efficiency of Al-5Ti-1B observed in the present experiment appears to be well below the normal acceptance level (220 μm average grain size) in standard TP-1 tests for inoculated Al-alloys [1]. In order to ensure reproducibility of the observed results, chemical grain refinement experiments were repeated several times with two different batches of the master alloy, all

resulting in similar grain size distribution in the solidified ingots. It is thought that the slower cooling rate in the present experiments, as compared to the cooling conditions for standard TP-1 grain refinement test, resulted in the larger than anticipated grain size. There could also be prominent recalescence at such slow cooling reducing the effectiveness of the chemical refiner.

The ingots solidified under ultrasonication revealed very effective microstructural refinement with uniform and equiaxed grain structure forming throughout the ingot. The measured average grain size varied between 168 ±19 μm at the top (near the ultrasonic horn) to 271 ±44 μm at the bottom edge of the ingot. The extent of grain refinement is far superior to the observed chemical refinement in most parts of the ingot, especially in the region surrounding the ultrasonic horn, as shown in Figs. 3 and 4. Only towards the edge of the ingot, chemical refinement produced grain size comparable to ultrasonic induced refinement. Using ultrasonication in conjunction with chemical inoculation consistently produced the finest grain structure in the ingots, better than the refinement achieved using either chemical refinement or ultrasonication in isolation. Throughout the ingot, the average grain size measured is below 200 μm with the finest grains forming near the ultrasonic horn with an average size of 130 ±16 μm.

### *3.2 Solidification microstructure in the Al-10% Cu ingots*

Microstructural examination of the Al-10% Cu alloy ingots revealed similar trends in grain refinement as observed for CP-Al. However, certain differences were noted as will be indicated below. Optical micrographs from samples solidified from 725 $^{o}$C under identical cooling rates but different melt treatment are shown in Fig. 5.

The measured average grain sizes in different ingots are presented in Fig. 6 as a function of distance from the top along the central vertical axis. For all experiments, the grain sizes observed in the alloy ingots are finer than those obtained in CP-Al under comparable processing conditions. Without any refining (inoculation or ultrasonication), large equiaxed dendritic grains with well-defined secondary arms are observed (Fig. 5a) throughout the base ingot. However, the grains are considerably smaller than those observed in the base CP-Al ingots with an average size of 717 ±79 μm. Chemical grain refinement using an Al-5Ti-1B master alloy triggered a drastic transformation to fine equiaxed grain structure in the entire ingot as shown in Fig. 5b. The variation in grain size with distance is minimal. Stronger refinement effect is noticed in the alloy as compared to CP-Al with an average grain size measured around 132 ±17 μm in the entire ingot.

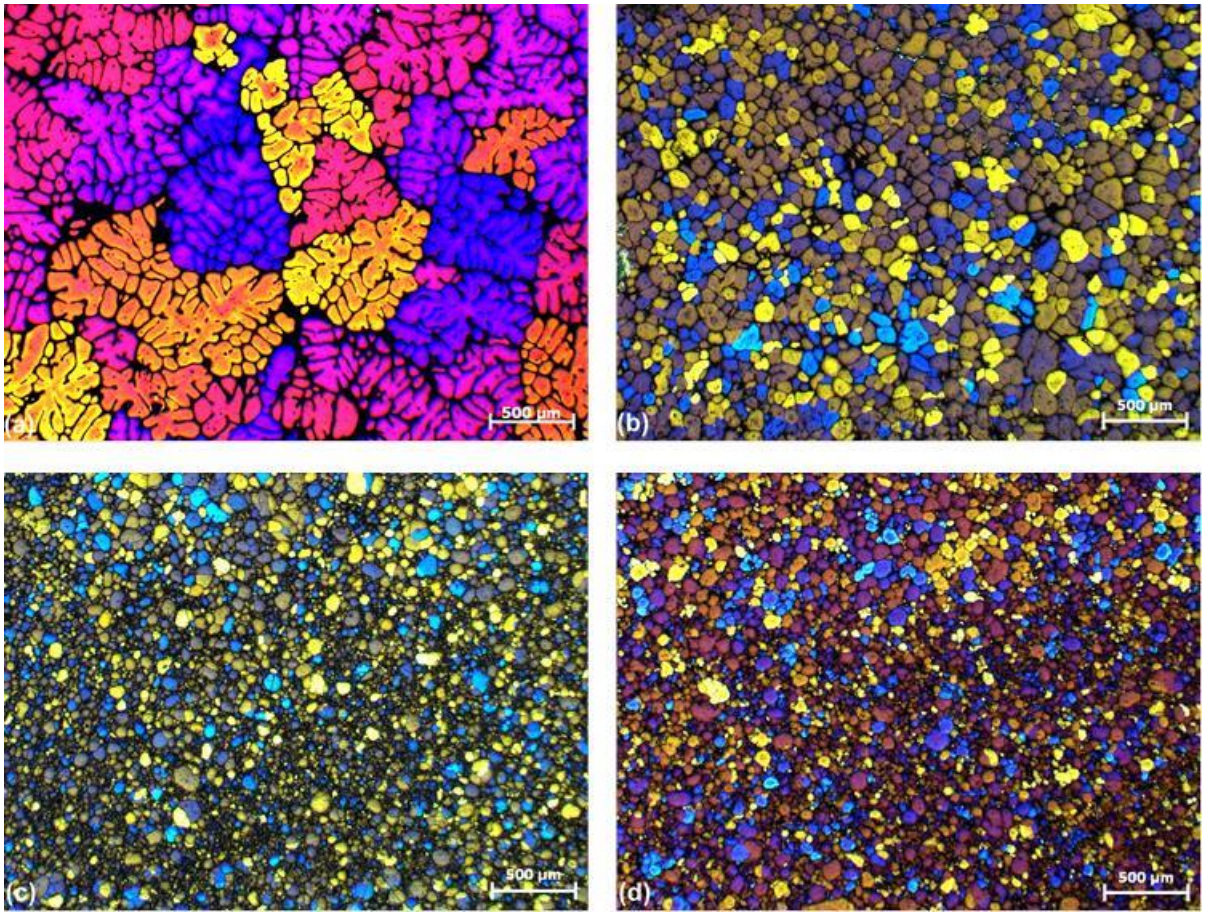


*Fig 5. Optical micrographs from Al-10%Cu alloy ingots cast under various conditions: (a) conventionally cast (b) Al-5Ti-1B inoculated (c) Ultrasonicated (d) Inoculated and ultrasonicated. All samples were cast at 725 °C.*

Ultrasonication during solidification, with or without chemical inoculation, leads to strong refinement in grain structure throughout the entire ingots as shown in Figs. 5 and 6. As observed with CP-Al samples, the finest grains are formed just below the horn where the acoustic energy transfer is the greatest. There is a progressive increase in the grain size with the axial distance from the horn due to the attenuation of ultrasound through the melt. Nevertheless, Fig. 6 indicates that the average grain size in the ultrasonicated samples remained consistently lower than the chemically inoculated ingots, even in the least refined section of the ingots. Surprisingly, in contrast to the observations for CP-Al, combining chemical inoculation with ultrasonication did not further refine the grain size of the alloy ingots over only ultrasonication (Figs. 5c and 5d). Fig. 6 clearly shows that the measured average grain size in the ultrasonicated ingots have comparable values in each section irrespective of chemical inoculation.

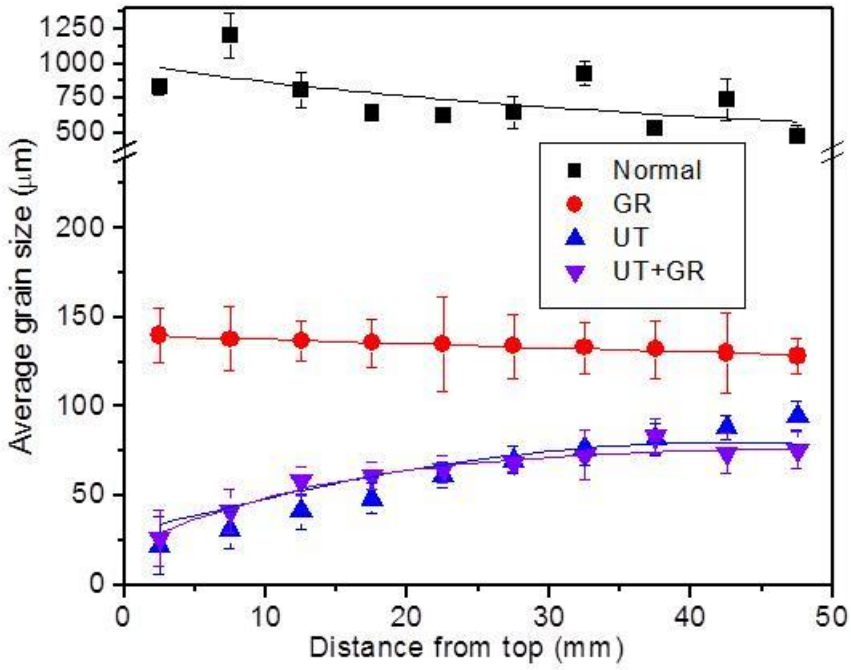


*Fig. 6. Measured average grain size for Al-10%Cu alloy ingots as a function of distance from the top along the central vertical axis. For ultrasonicated samples distance is measured from the tip of the radiator.*

Table 2 summarises the average grain sizes measured in ingots solidified under different treatments keeping the cooling conditions identical. The results corroborate the microstructural observation.

*Table 2. Average grain size data measured from the CP-Al and the Al-10%Cu ingots solidified under different condition. Microstructure throughout the ingot is used for the size measurement. SDAS represents the secondary dendrite arm spacing.*

| Refining method | Commercial purity Al | | | Al-10wt.%Cu Alloy | | | | |
|---|---|---|---|---|---|---|---|---|
| | Average Grain size (μm) | SDAS (μm) | Grain density ($mm^{-3}$) | Cooling rate ($^oCmin^{-1}$) | Average Grain size (μm) | SDAS (μm) | Shape factor | Grain density ($mm^{-3}$) |
| Base alloy | 6730 ± 627 | 372 | <<1 | 42 | 717 ± 79 | 86 | □ | 5 |
| Al-5Ti-1B (GR) | 287 ± 48 | □ | 81 | 42 | 132 ± 17 | □ | 0.7 | 836 |
| Ultrasonic (UT) | 233 ± 37 | □ | 150 | 50 | 65 ± 25 | □ | 0.8 | 7052 |
| GR + UT | 169 ± 34 | □ | 395 | 48 | 63 ± 17 | □ | 0.8 | 7711 |

For any specific treatment, Al-10% Cu alloy produced finer grain size compared to CP-Al. Both grain refiner addition and ultrasonication promoted considerable refinement and equiaxed non-dendritic grain structure under the natural cooling conditions of the present experiments. However, the results clearly demonstrate superior physical grain refinement under ultrasonication compared to the widely-practiced conventional chemical inoculation for Al-alloys. While the addition of chemical refiner further improved the refining efficiency of ultrasonication for CP-Al, in the Al-10% Cu alloy this did not promote noticeable change in the average grain size (63 ±17 μm vs 65 ±25 μm). Table 2 also reports the average grain densities calculated in ingots assuming a space-filling geometry of spherical grains. The results are much more revealing, than the grain size alone, in comparing the refinement efficiency of ultrasonication to the traditional chemical refinement. While a large increase in grain density resulted from chemical inoculation of the base CP-Al, ultrasonication alone shows a further ~100% increase in grain density over chemical grain refinement. Combining both the chemical refiner and the ultrasonication increased the grain density to almost five times over that of chemical inoculation. In the case of the Al-10% Cu alloy, ultrasonication clearly shows much higher refining efficiency with an eight times increase in grain density over chemical inoculation. There is a nominal further increase in the grain density by combining chemical grain refiner with ultrasonication. The calculated average shape factor of the grains is also reported in Table 2, with a value of 1 indicating a perfectly spherical particle. A higher value for the shape factor of the grains after ultrasonication compared to inoculation suggests a more equiaxed nature of the grains formed under ultrasonication.

### *3.3 Origin of grain refinement in the ultrasonicated ingots*

The average ultrasound energy transmission rate through a unit propagation area is expressed as [14],

$I = ½ \rho c (2\pi f A)^2$

where, $\rho$ is the density of the melt, $c$ the propagation velocity of sound, $f$ and $A$ the frequency and the amplitude of ultrasound, respectively. Estimating $c$ as $1.3 \times 10^3$ $ms^{-1}$ [14] and $\rho_{AL}$ as 2.385 $g/cm^3$ [27], energy transmission in the present experiment can be calculated as 1500 $Wcm^{-2}$ for an amplitude of 25 μm. This is well above the reported cavitation threshold of 100 $Wcm^{-2}$ in Al melt [14]. Moreover, inclusions in commercial purity melt are stated to reduce the cavitation threshold further [23]. Developed cavitation is thus expected in the ultrasonicated melts and semi-liquid slurry and likely responsible for the observed physical refinement of microstructure.

It should be noted that soluble Ti has a strong growth restriction effect in Al-melt. There is a possibility of Ti dissolution from the horn contributing to the observed grain refinement in the ultrasonicated Al-melt. Compositions determined through optical emissions spectroscopy of Al-10% Cu alloy ingots processed under different conditions are presented in Table 3. Ti concentration varied between different ultrasonicated ingots and the observed range of concentration is given for various regions in the ingots. Although no visible degradation of the horn was observed, Ti pickup in the melt under ultrasonication is noted especially close to the horn. This would contribute growth restriction of solid particles near the horn. However, the growth restriction and constitutional undercooling alone does not fully explain the high grain density in the absence of potent nucleants under ultrasonication. Most importantly, a higher level of soluble Ti, along with highly potent nucleant particles, is present in the chemically inoculated ingot. Yet the extent of chemical grain refinement is inferior to the physical refinement in ultrasonicated ingots. Therefore, the observed grain refinement is thought to be contributed by other factors rather than soluble Ti under ultrasonication.

*Table 3. Composition of Al-10wt.%Cu alloy ingots solidified under different conditions as determined through optical emissions spectroscopy.*

| Processing Condition | Elemental concentration (wt.%) | | | | |
|---|---|---|---|---|---|
| | Al | Si | Fe | Cu | Ti |
| Unrefined | balance | 0.04 | 0.147 | 9.8 | 0.003 |
| Grain refined | balance | 0.04 | 0.147 | 9.9 | 0.12 |
| Ultrasonicated (near horn) | balance | 0.04 | 0.147 | 9.8 | 0.06 - 0.09 |
| Ultrasonicated (middle of ingot) | balance | 0.04 | 0.147 | 9.8 | 0.03 – 0.05 |
| Ultrasonicated (bottom of ingot) | balance | 0.04 | 0.147 | 9.8 | 0.01 - 0.02 |

The cooling rates measured from the linear sections of the cooling curves under different treatment conditions are presented in Table 2 for the Al-10% Cu alloy. Ultrasonication increases the overall cooling rate but not drastically to account for the observed grain refinement compared to the base alloy. However, significant slowing down of the cooling rates for the cases of chemical inoculation and ultrasonication is observed just before recalescence with cooling rates of 41, 36, 32 and 34 K $min^{-1}$ for the base alloy, chemical inoculation, ultrasonication and combined refinement, respectively. This may indicate increased nucleation activity under chemical inoculation and

ultrasonication. Figure 7 compares enlarged sections of the cooling curves relevant to α-Al solidification in the Al-10% Cu ingot samples under different treatment conditions. Increased noise seen in the curves for the ultrasonicated samples is due to the proximity of the thermocouple to the horn, but the general trends of solidification can be observed. As expected, base alloy shows largest melt undercooling with a minimum temperature recorded at 618.5 $^{o}$C. On chemical inoculation, there is a prominent decrease in the maximum undercooling with a minimum recorded melt temperature of 623 $^{o}$C. Ultrasonication indicates a maximum melt undercooling comparable to chemical inoculation with a recorded minimum also at 623 $^{o}$C. That chemical refiner addition did not contribute to further refinement under ultrasonication is also substantiated by the identical nature of the cooling curves recorded in both cases of sonication. This suggests that heterogeneous nucleation under ultrasonication could be as effective as inoculation through Al-5Ti-1B chemical refiner.

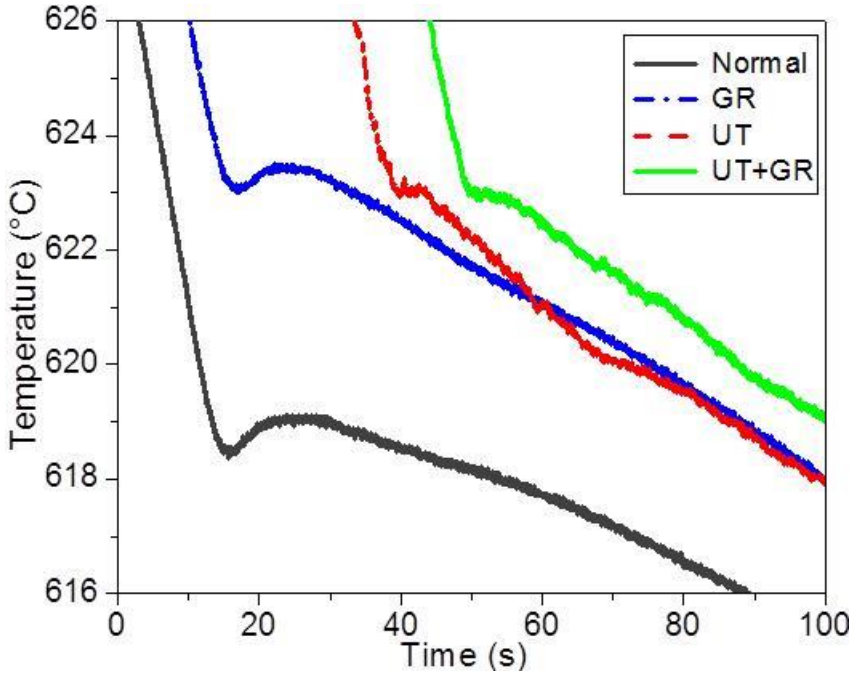


*Fig. 7. Enlarged sections of the measured cooling curves from Al-10wt.% Cu ingots solidified under different conditions illustrating formation of α-Al grains. GR, UT and UT+GR represent chemical inoculation, ultrasonication and combined ultrasonic and chemical inoculation, respectively.*

## 4. Discussion

Two key mechanisms are generally attributed to grain refinement under ultrasonication; dendrite fragmentation and enhanced nucleation. As ultrasonication was performed during

solidification, mechanical fragmentation of dendrites is possible under cavitation. Dendrite fragmentation may also occur through local changes in the temperature or solute concentration from the convective fluid flow [28]. Cavitation induced fragmentation of well-developed dendrites has previously been observed in non-metallic analogue system [29]. Strong fluid flow through acoustic streaming can strip growing dendrites from the substrate, carry them into the region of cavitation, and distribute dendrite fragments in the bulk melt. Refinement of the entire ingot grain structure is then possible through enough fragmentation, distribution and survival of such fragments leading to grain multiplication.

In the present experiments, grain sizes observed even furthest from the ultrasonic radiator is finer than in chemical inoculation. Also, no remains of primary dendrite stems or coarse grains resulting from them are observed in the entire ultrasonicated ingot. Considering the similar cooling conditions, secondary dendrite arm spacing (SDAS) in the unrefined ingots was compared against the grain size of the ultrasonicated ingots to check if fragmentation of secondary arms is responsible for the observed refinement. Table 2 reports the measured average SDAS of 372 μm for CP-Al and 86 μm for Al-10%Cu alloy base ingots. Under comparable cooling environment, the measured average grain sizes of 233 μm and 65 μm in the ultrasonicated CP-Al and Al-10%Cu ingots are finer than the respective SDAS. Therefore, fragmentation of well-developed dendrites seems unlikely contributor to the observed grain refinement. To explain the fine equiaxed microstructure on the basis of fragmentation would require predominant fragmentation during very early stage of dendrite evolution and subsequent survival and crowding of such fragments in the melt. If such small and mobile early dendrites substantially fragment under cavitation needs to be investigated in metallic systems.

On the other hand, prominent reduction of nucleation undercooling under ultrasonication in Fig.7 suggests enhanced heterogeneous nucleation. Discounting evaporative melt undercooling at the bubble-melt interface [25], enhanced nucleation under ultrasonication can be attributed to two possible mechanisms as discussed below. Forced wetting of the endogenous substrates such as the mould wall and non-metallic inclusions have been argued to increase heterogeneous nucleation sites under cavitation. However, the lack of grain refinement observed in melt solidified following ultrasonication above the liquidus [30] contradicts this proposition. Moreover, these nucleation sites are significantly less potent than the nucleants in chemical refiner. Yet ultrasonication produced better refinement than inoculation in both CP-Al and Al-10%Cu ingots. Potency of heterogeneous nucleation sites can be assessed from the required nucleation undercooling. Highly potent nucleants drastically reduce melt

undercooling such as $TiB_2$ in Al-5Ti-1B inoculated Al-melt initiating heterogeneous nucleation at undercooling as low as 0.2 $^oC$ [31]. The observation of similar melt undercooling under inoculation and ultrasonication in Fig. 7 is inexplicable from potency of nucleating sites.

The small quantity of latent heat liberated at the beginning of nucleation is generally masked by the high rate of heat extraction from the solidifying melt. Thus, initiation of nucleation is better estimated from the first deflection in the cooling curve rather than the recorded maximum undercooling. The nucleation initiation temperatures in the present experiments have been estimated from the first derivative of temperature with time (deflection in the slope) in the cooling curves presented in Fig. 7. Nucleation temperatures of 620, 625, 624 and 625 $^oC$ have been estimated for the base, chemically inoculated, and ultrasonicated melts without and with refiner addition, respectively. Clearly, ultrasonication reduced actual nucleation temperature by 5 $^oC$ over conventional solidification indicating enhancement of heterogeneous nucleation under cavitation. The slightly higher nucleation temperature under inoculation over only ultrasonication corroborates higher potency of nucleants from inoculation. Nevertheless, the observed increase in the nucleation temperature (and better grain refinement) under ultrasonication cannot be explained purely on the basis of forced wetting of low-potency natural substrates under cavitation.

An alternative mechanism of pressure induced shift of the equilibrium temperature has been proposed [25, 26] and used as a plausible explanation for enhanced nucleation under cavitation in metallic melts [15, 32]. As metallic melts contract on solidification, cavitation generated pressure pulse can increase the equilibrium freezing point as suggested by the Clapeyron equation,

$$\Delta P = \frac{L}{\mathrm{T_m}\Delta V}\,\Delta T$$

where $\Delta P$ is the increased pressure, $L$ the latent heat of freezing, $\Delta V$ the change in volume upon solidification, $T_m$ the equilibrium freezing point and $\Delta T$ the change in the freezing point. For CP-Al, $\Delta T$ can be calculated using parametric values reported in Ref. [27]: $L$ = 3.88 x $10^5$ J/kg and density of liquid Al at the freezing point ($T_m$ = 933.47 K) being 2.385 g/cm$^3$. From the reported values of thermal expansion co-efficient at different temperature ranges [33], a 4.9% volume expansion of solid Al is calculated for temperature increase from 20 $^oC$ to the freezing point. The density of solid Al at the freezing point can then be estimated to 2.574 g/cm$^3$ from the calculated volume expansion and the reported density of 2.7 g/cm$^3$ at 20 $^oC$. Accordingly, at $T_m$, $\Delta V$ = − 3.08 x $10^{-5}$ m$^3$ per kg of Al. At a distance twice the radius of a collapsing bubble, the pressure pulse vary between 200 – 1000 atm (≈

$2x10^7$ – $10^8$ Pa) [14]. The corresponding rise in the equilibrium freezing point can be estimated between 1.5 – 7.4 $^oC$. In other words, under identical cooling conditions and melt temperature, CP-Al melt can experience an effective local undercooling of up to 7.4 $^oC$ under ultrasonication over conventional solidification. The shift of the liquidus for the Al-10%Cu alloy could not be estimated due to unavailability of necessary data though an increase is expected. This increase of freezing point provides additional undercooling to activate low-potency nucleants. Therefore, cavitation induced shift of the freezing point in conjunction with the forced wetting of substrates explains the reduction in nucleation undercooling and grain refinement under ultrasonication in the present study. Although there is no direct evidence yet supporting this hypothesis, an in-situ small angle X-ray scattering (SAXS) investigation suggests cavitation enhanced nucleation in an Al-15wt.% Cu alloy melt above its liquidus temperature [34].

Despite the enhanced heterogeneous nucleation under ultrasonication, the large increase in grain number density compared to chemical inoculation (Table 2) needs further explanation. Although Al-5Ti-1B inoculation utilises more potent heterogeneous nucleation sites, ultrasonication seems to have nucleated more grains. Similar observation has been reported in Mg-alloys [15]. One should note that only 0.1–1% of the potent nucleants contribute to grain formation in inoculated Al- and Mg-alloys [2, 15]. While efficient refiners initiate nucleation at extremely low undercooling, only the largest size particles act as transformation nuclei leading to free growth [2]. An estimate for Al shows the minimum size of $TiB_2$ particle actively contributing to grain formation to be 3 μm [2]. Majority of the nucleants (~99%) with smaller particle size do not contribute to grain formation as the release of latent heat (recalescence) lowers melt undercooling. Figure 7 clearly shows distinct recalescence following nucleation in the base and chemically inoculated ingots in the present experiment. In contrast, ultrasonicated ingots do not indicate any prominent recalescence in Fig. 7 due to efficient dissipation of the latent heat under the intense convection. A favourable situation for prolonging nucleation and a larger fraction of the available nucleants can then contribute to grain formation as compared to chemical inoculation. This explains the higher grain density observed in the present study under ultrasonication even though inoculation ulitilises more potent nucleants.

Another important observation from the present experiments is the large reduction in grain size (or increase in grain density) under ultrasonication in the Al-10% Cu alloy as compared to CP-Al. This is expected due to the growth restriction and constitutional undercooling effect of solute under quiet solidification condition. Also, chemical inoculation of the Al-10% Cu alloy did not substantially

improve the refinement effect of ultrasonication, indicating high nucleation efficiency under ultrasonication alone. The general perception is that strong fluid flow under cavitation may homogenise solute distribution at the solid-liquid interface reducing the constitutional undercooling effect. However, presence of solute appears to further enhance the grain refining effect of ultrasound and this effect needs further investigation.

It should be noted that while the indirect evidence from the present experiment suggests enhanced nucleation being a major contributor to grain refinement under ultrasonication, dendrite fragmentation may also operate depending on the solidification conditions. Direct observation of grain formation under cavitation may clarify the conditions under which each of these mechanisms dominate.

## 5. Conclusions

Microstructural refinement in CP-Al and Al-10 wt.% Cu alloy is examined under ultrasonication and compared against Al-5Ti-1B inoculation under identical natural air cooling.

Both inoculation and ultrasonication refined the coarse dendritic microstructure of the base ingots into fine equiaxed grain structure. Inoculated ingots showed finest grains near the mould wall while ultrasonicated ingots displayed best refinement at the top (just below the radiator).

Ultrasonication produced better refinement than inoculation in both CP-Al and Al-10 wt.% Cu with ~8 times increase in the grain density in the alloy. Combining ultrasonication with inoculation resulted in the finest grain structure in CP-Al but the effect for Al-10 wt.% Cu was marginal.

Cooling curves measured under ultrasonication and inoculation show similar reduction in the nucleation undercooling compared to the unrefined base ingots. However, distinct recalescence observed in the inoculated melt was largely eliminated in the ultrasonicated melts.

Indirect evidence suggests major contribution from enhanced heterogeneous nucleation in the present experiments presumably from pressure induced shift of freezing point.

Larger number of grain initiation from enhanced and prolonged nucleation is proposed under ultrasonication explaining the observed superior refinement despite chemical inoculation having better potency nucleants.

**References**


[1] B.S. Murty, S.A. Kori, M. Chakraborty, Grain refinement of aluminium and its alloys by heterogeneous nucleation and alloying, Int. Mater. Rev. 47 (2002) 3-29.

[2] A.L. Greer, P.S. Cooper, M.W. Meredith, W. Schneider, P. Schumacher, J.A. Spittle, A. Tronche, Grain refinement of aluminium alloys by inoculation, Adv. Eng. Mater. 5 (2003) 81-91.

[3] D.H. StJohn, M. Qian, M.A. Easton, P. Cao, Z. Hildebrand, Grain refinement of magnesium alloys, Metall. Mater. Trans. A, 36 (2005) 1669-1679.

[4] J.A. Spittle, Columnar to equiaxed grain transition in as solidified alloys, Int. Mater. Rev. 51 (2006) 247-269.

[5] M.A. Easton, M. Qian, A. Prasad, D.H. StJohn, Recent advances in grain refinement of light metals and alloys, Curr. Opin. Solid State Mater. Sci. 20 (2016) 13–24

[6] D. Qiu, J.A. Taylor, M-X. Zhang, P.M. Kelly, A mechanism for the poisoning effect of silicon on the grain refinement of Al–Si alloys, Acta Mater. 55 (2007) 1447–1456.

[7] C. Limmaneevichitr, W. Eidhed, Fading mechanism of grain refinement of aluminum–silicon alloy with Al–Ti–B grain refiners, Mater. Sci. Eng. A, 349 (2003) 197–206.

[8] A.M. Bunn, P. Schumacher, M.A. Kearns, C.B. Boothroyd, A.L. Greer, Grain refinement by Al–Ti–B alloys in aluminium melts: a study of the mechanisms of poisoning by zirconium, Mater. Sci. Tech. 15 (1999) 1115-1123.

[9] A.M. Detomi, A.J. Messias, S. Majer, P.S. Cooper, The imact of TiCAl and TiBAl grain refiners on cast house processing, in: Light Metals, J.L. Anjier (Ed.), TMS, New Orleans, LA, 2001, pp.919-925.

[10] A. Das, G. Liu, Z. Fan, Investigation on the microstructural refinement of an Mg–6 wt.% Zn alloy, Mater. Sci. Eng. A, 419 (2006) 349-356.

[11] M. Li, T. Tamura, K. Miwa, Controlling microstructures of AZ31 magnesium alloys by an electromagnetic vibration technique during solidification: from experimental observation to theoretical understanding, Acta Mater. 55 (2007) 4635-4643.

[12] D. Räbiger, Y. Zhang, V. Galindo, S. Franke, B. Willers, S. Eckert, The relevance of melt convection to grain refinement in Al–Si alloys solidified under the impact of electric currents, Acta Mater. 79 (2014) 327-338.

[13] K. Kocatepe, C.F. Burdett, Effect of low frequency vibration on macro and micro structures of LM6 alloys, J Mater. Sci. 35 (2000) 3327-3335.

[14] G.I. Eskin, Ultrasonic treatment of light alloy melts, Gordon and Breach, 1998.

[15] A. Ramirez, M. Qian, B. Davies, T. Wilks, D.H. StJohn, Potency of high-intensity ultrasonic treatment for grain refinement of magnesium alloys, Scripta Mater. 59 (2008) 19-22.

[16] M. Qian, A. Ramirez, A. Das, Ultrasonic refinement of magnesium by cavitation: clarifying the role of wall crystals, J. Cryst. Growth, 311 (2009) 3708-3715.

[17] V. Abramov, O. Abramov, V. Bulgakov, F. Sommer, Solidification of aluminium alloys under ultrasonic irradiation using water-cooled resonator, Mater. Lett. 37 (1998) 27-34.

[18] G.I. Eskin, Broad prospects for commercial application of the ultrasonic (cavitation) melt treatment of light alloys, Ultrasonic Sonochemistry, 8 (2001) 319-325.

[19] X. Xian, T.T. Meek, Q. Han, Refinement of eutectic silicon phase of aluminum A356 alloy using high-intensity ultrasonic vibration, Scripta Mater. 54 (2006) 893-896.

[20] C. Ruirun, Z. Deshuang, G. Jingjie, M. Tengfei, D. Hongsheng, S. Yanqing, F. Hengzhi, A novel method for grain refinement and microstructure modification in TiAl alloy by ultrasonic vibration, Mater. Sci. Eng. A, 653 (2016) 23-26.

[21] S.V. Komarov, M. Kuwabara, O.V. Abramov, High Power ultrasonics in pyrometallurgy: current status and recent development, ISIJ International 45 (2005) 1765-1782.

[22] X. Li, T. Li, X. Li, J Jin, Study of ultrasonic melt treatment on the quality of horizontal continuously cast Al–1%Si alloy, Ultrasonic Sonochemistry, 13 (2006) 121-125.

[23] G.I. Eskin, D.G. Eskin, Production of natural and synthesized aluminum-based composite materials with the aid of ultrasonic (cavitation) treatment of the melt, Ultrasonic Sonochemistry, 10 (2003) 297-301.

[24] Y. Tsunekawa, H. Suzuki, Y. Genma, Application of ultrasonic vibration to in situ MMC process by electromagnetic melt stirring, Mater. Des. 22 (2001) 467-472.

[25] B. Chalmers, Principles of Solidification, John Wiley & Sons, NY, 1964, pp. 86-89.

[26] J.D. Hunt, K.A. Jackson, Nucleation of Solid in an undercooled liquid by cavitation, J. Appl. Phys. 37 (1966) 254-257.

[27] E.A. Brandes, G.B. Brooke (Eds.), Smithells Metals Reference Book, Butterworth-Heinemann, OX, 1992.

[28] A. Hellawell, S. Liu, S.Z. Lu, Dendrite fragmentation and the effects of fluid flow in castings, JOM 49 (1997) 18-20.

[29] D. Shu, B. Sun, J. Mi, P.S. Grant, A high-speed imaging and modeling study of dendrite fragmentation caused by ultrasonic cavitation, Metall. Mater. Trans. A, 43 (2012) 3755-3766.

[30] G. Wang, M.S. Dargusch, M. Qian, D.G. Eskin, D.H. StJohn, The role of ultrasonic treatment in refining the as-cast grain structure during the solidification of an Al–2Cu alloy, J Cryst. Growth, 408 (2014) 119-124.

[31] A.L. Greer, Grain refinement of alloys by inoculation of melts, Phil. Trans. R. Soc. Lond. A 361 (2003) 479-495.

[32] A. Das, H.R. Kotadia, Effect of high-intensity ultrasonic irradiation on the modification of solidification microstructure in a Si-rich hypoeutectic Al–Si alloy, Mater. Chem. Phys. 125 (2011) 853-859.

[33] E.A. Brandes, G.B. Brooke (Eds.), Smithells Light Metals Handbook, Butterworth-Heinemann, OX, 1998.

[34] H. Huang, D. Shu, J. Zeng, F. Bian, Y. Fu, J. Wang, B. Sun, In situ small angle X-ray scattering investigation of ultrasound induced nucleation in a metallic alloy melt, Scripta Mater. 106 (2015) 21-25.